

## Germanium nanowires grown using different catalyst metals



R.C. Gouveia<sup>a, b, \*</sup>, H. Kamimura<sup>a</sup>, R. Munhoz<sup>a</sup>, A.D. Rodrigues<sup>a</sup>, E.R. Leite<sup>c</sup>, A.J. Chiquito<sup>a</sup>

<sup>a</sup> Departamento de Física – Nano Lab, Universidade Federal de São Carlos, Rod. Washington Luís, Km 235 – SP 310, São Carlos, CEP 13565-905, Brazil

<sup>b</sup> Área de Ciências, Instituto Federal de Educação Ciência e Tecnologia de São Paulo, Rua Américo Ambrósio, 269, Jd. Canaã, Sertãozinho, CEP 14169-263, Brazil

<sup>c</sup> Departamento de Química – LIEC, Universidade Federal de São Carlos, São Carlos, CEP 13565-905, Brazil

### HIGHLIGHTS

- Ge nanowires were grown by VLS method using Au, Ag, Cu, In and Ni as catalysts.
- All nanowires presented high single crystalline quality and long range order.
- Devices showed semiconducting behavior having VRH as dominant transport mechanism.
- The metal catalyst did not influence structural properties or the transport mechanism.

### ARTICLE INFO

#### Article history:

Received 1 October 2015

Received in revised form

4 August 2016

Accepted 6 August 2016

Available online 7 August 2016

#### Keywords:

Nanostructures

Semiconductors

Raman spectroscopy

Transport properties

### ABSTRACT

Germanium nanowires have been synthesized by the well known vapor-liquid-solid growth mechanism using gold, silver, copper, indium and nickel as catalyst metals. The influence of metal seeds on nanowires structural and electronic transport properties was also investigated. Electron microscopy images demonstrated that, despite differences in diameters, all nanowires obtained presented single crystalline structures. X-ray patterns showed that all nanowires were composed by germanium with a small amount of germanium oxide, and the catalyst metal was restricted at the nanowires' tips. Raman spectroscopy evidenced the long range order in the crystalline structure of each sample. Electrical measurements indicated that variable range hopping was the dominant mechanism in carrier transport for all devices, with similar hopping distance, regardless the material used as catalyst. Then, in spite of the differences in synthesis temperatures and nanowires diameters, the catalyst metals have not affected the composition and crystalline quality of the germanium nanowires nor the carrier transport in the germanium nanowire network devices.

© 2016 Elsevier B.V. All rights reserved.

### 1. Introduction

Semiconductor nanowires attract the interest of scientists because of their wide range of potential applications, such as electronic, photonic, energy and magnetic [1]. Germanium has been receiving special attention as a precursor material in nanostructure manufacturing due to its particular characteristics: high carrier mobility and compatibility with conventional silicon equipments, favoring electronic applications; narrow indirect (0.66eV) and direct (0.8eV) bandgaps, supporting optical devices

development in infrared and visible regions; and large excitonic Bohr radius (24.3 nm), highlighting quantum size effects [2,3].

Different experimental methods have been used for obtaining germanium nanowires (GeNWs) such as vapor-liquid-solid (VLS), vapor-solid-solid (VSS) and solution-liquid-solid (SLS) [4]. Among these techniques, the most widely used is the VLS mechanism which relies on a vapor phase precursor of the nanowire material being adsorbed onto a liquid seed and then precipitating at the growth surface, resulting in nanostructures [2,5,6].

In this technique, gold is generally used as catalyst seed, but recent papers have reported investigations of the growth of GeNWs using different catalyst metals. Barth et al. [7] and Biswas et al. [8] studied the use of Ag as growth seed for generating GeNWs via SLS. Kang et al. [9] and Geaney et al. [10] reported a VSS growth of GeNWs using Cu-catalysts. Lu et al. [11] and Thombare et al. [12] studied SLS and VSS Ni-seeded synthesis of GeNWs, respectively.

\* Corresponding author. Departamento de Física – Nano Lab, Universidade Federal de São Carlos, Rod. Washington Luís, Km 235 - SP 310, São Carlos, CEP 13565-905, Brazil.

E-mail address: [riama@ifsp.edu.br](mailto:riama@ifsp.edu.br) (R.C. Gouveia).

Xiang et al. [13] presented a route for GeNWs by In-seeded VLS growth. Furthermore, some authors have discussed the use of other possible catalyst metals such as Bi, Sn and Mn [4].

Despite the great contribution to the understanding of growth process and nanowires properties achieved in each one of these publications, they present different routes for the synthesis of GeNWs making difficult a comparative analysis of how the seed metals influence the nanowire's properties. Therefore, the aim of this study was to provide a comparison between the nanowires growth by the same method (VLS) but using different catalysts (Au, Ag, Cu, In and Ni) regarding to structural characteristics and transport mechanisms. The use of these metals can provide a good overview of this subject, since they have metal-Ge eutectic curves characterized by distinct features, as well as different diffusion coefficients and energy levels in germanium crystals.

## 2. Synthesis and characterization of the nanowire networks

Initially, thin films of gold, silver, copper, indium and nickel were deposited on Si/SiO<sub>2</sub> (oxide layer 500 nm thick) substrates under high vacuum (better than 10<sup>-6</sup> mbar). Then, in order to generate the catalyst nanoparticles the substrates with thin (2 nm) metallic films were submitted to thermal treatment under temperatures of 600 °C for Au and Cu and 800 °C for Ag and Ni. For In-based growth the film was 1 nm thick and the thermal treatment was not used.

The synthesis was carried out in a tube furnace system (Lindberg/Mini Mite) where high purity germanium powder (Aldrich, purity > 99.999%) was placed at the center of the furnace and heated to 950 °C. Previously prepared substrates were placed at specific positions with temperatures of 800 °C for Ag, Cu and Ni nanoparticles and 600 °C for Au seeds and In film. All these temperatures are higher than the eutectic point for used metal-Ge alloys. Argon (White Martins, purity > 99.998%) was used for carrying the Ge vapor to the substrates during growth. After 1 h of synthesis the furnace was turned off and naturally cooled to room temperature.

Hereafter, the composition of resultant nanowire networks was analyzed by X-ray diffraction (Shimadzu, XRD 6100, 40 kV, 30 mA, Cu K $\alpha$  radiation) and Raman spectroscopy; also the nanowires' dimensions were statistically studied using images taken by scanning electron microscopy (SEM, JEOL JSM 6510) and field emission scanning electron microscopy (FEG-SEM, Zeiss Supra 35). Raman scattering experiments were performed in a triple grating spectrometer equipped with microscope facilities. Liquid nitrogen cooled CCD was used as detector. Spectrometer slits were adjusted in order to provide a spectral resolution of 1.5 cm<sup>-1</sup>. The line 514.5 nm of an argon laser was used as excitation source with a controlled power lower than 1 mW, in order to avoid heating of the samples. All measurements were performed keeping the same experimental parameters.

An initial inspection of the as-grown samples by XRD and Raman spectroscopy indicates that the structures are composed mainly of crystalline germanium with a small amount of germanium oxide, without significant presence of any other compounds.

XRD patterns of samples grown using different metal seeds are shown in Fig. 1(a) where it is possible to observe the peaks (111), (220) and (311) of germanium, agreeing with the powder diffraction card PDF 4–545 [14] which corresponds to a diamond structure (space group Fd-3m). GeO<sub>2</sub> peaks with a hexagonal structure in accordance with PDF 36–1463 diffraction card [15] were also detected, mostly for GeNWs synthesized at higher temperatures (using Ag, Cu and Ni nanoparticles); this germanium oxide could be located in the nanowires, possibly forming a shell [5], or in the microcrystals present in the growth substrates.

In agreement with x-ray analyses, Raman spectra [Fig. 1(b)]

taken from all samples presented pronounced peaks centered at 300 cm<sup>-1</sup>, attributed to Ge optical phonons. The spectra measured from the samples grown with Au, Ag, Cu and Ni also show peaks with wave numbers around 443 cm<sup>-1</sup> related to the A<sub>1</sub> vibration of the  $\alpha$ -quartz phase of native GeO<sub>2</sub> [16] present in the substrates. This feature cannot be found in the spectra of the sample prepared using indium and gold nanoparticles, as an indication that no significant volume of germanium oxide was produced during the growth process at a lower temperature, which also agrees with XRD pattern.

Regarding the generation of the nanoparticles by treatment of previous evaporated thin metallic film, Fig. 2 (a and b) shows that the Au, Ag, Cu and Ni films produced catalyst seeds with dimensions and densities proper for nanowires synthesis. The differences in size and distribution of the nanoparticles on the substrates may be caused by differences in the physical properties of the metals such as melting point, viscosity, etc. Indium thin films were subjected to annealing process at a wide range of temperatures (70 °C–800 °C) and no nanoparticles were observed, probably due to the low melting point and high viscosity of this metal.

SEM and FEG-SEM images [Fig. 2(c)] revealed that in each type of sample there is a region covered by a high density of nanowires characterized by a large aspect ratio (~10<sup>3</sup>). Some variation in the nanowires morphology was also noticed, probably due to the differences in the density and distribution of the nanoparticles on the substrate [2]. For the same reason, in those substrates prepared with Cu, In and Ni thin films, the presence of microcrystals in addition to nanowires were observed; these structures are also composed of germanium and/or germanium oxide, as indicated in XRD and Raman analyses, which have not detected the presence of any other elements.

As expected from the VLS mechanism [17] and evidenced in histograms of Fig. 2 (b and d) the grown nanowires exhibited diameters distribution compatible with that of the corresponding metallic nanoparticles. By analyzing more deeply the data in the histograms in Fig. 2(a and c) one notice that the average of nanowire diameters ( $\bar{D}$ ) are higher for Ag catalyst (98.3 nm) and lower for Ni catalyst (18.2 nm), while for other metals in this study the mean value was found to be 55.9 nm (Au), 52.4 nm (Cu) and 89.1 nm (In). Concerning to the variance of the diameters, In-seeded GeNWs showed broadened cross-section distribution (standard deviation around 43.8 nm) since the synthesis was conducted using non-previously annealed thin film (instead of nanoparticles with defined sizes). On the other hand, nanowires grown from Ni nanoparticles are quite homogeneous in diameters, presenting a standard deviation ( $\sigma$ ) of only 6.6 nm. Gold and copper catalysts generated nanowires with similar distribution; the difference lies on the fact that for gold the quantity of nanowires with diameters larger than 90 nm is negligible but for copper a small portion of nanowires with diameters reaching 120 nm is still observed.

Therefore, despite the catalyst metal has not interfered in the composition of nanowires network, as shown by XRD and Raman analysis, considerable differences in the dimensions of nanostructures were produced, which possibly have influence on mechanical, optical and electronic properties.

## 3. Structural characterization of individual nanowires

For better understanding the crystalline parameters and composition of the nanowires that were grown using the five catalyst metals and investigating the influence of nanowire dimensions in vibrational properties, high resolution transmission electron microscopy (HRTEM, TecnaiF20G2, FEI, measurements at room temperature with an acceleration voltage of 200 kV, equipped

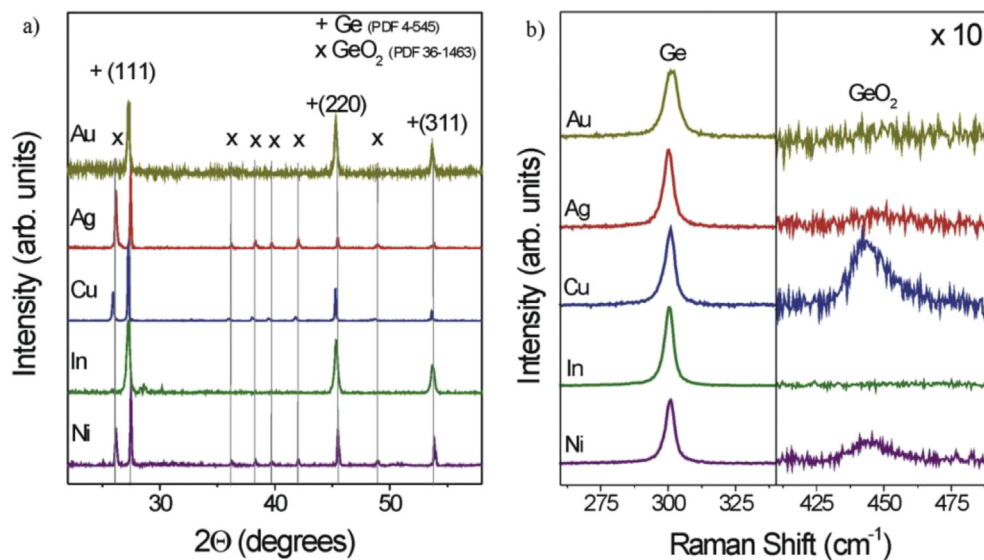


**Fig. 1.** (a) X-ray diffraction patterns of GeNWs, grown using Au, Ag, Cu, In and Ni as nucleation seeds, showing Ge (PDF 4–545) and  $\text{GeO}_2$  (PDF 36–1463) peaks. (b) Raman spectra of GeNWs. The left side shows pronounced peaks referring to germanium optical vibrations. The right side presents the spectral range of A1 vibrations in  $\text{GeO}_2$ .

with an energy-dispersive X-ray spectrometer EDS) and micro-Raman analysis of individual GeNWs were performed.

From HRTEM images and their respective Fast Fourier Transformations (FFT) obtained from samples grown using the five catalyst metals, the single crystalline nature of GeNWs and their preferential growth orientation ((111) direction) were observed. As examples, nanowires grown from Ag and In are depicted in Fig. 3(a) and (b), respectively, and Fig. 3(c) and (e) show their FFTs. The space between crystalline planes of the nanowires are compatible with germanium diamond structure with a lattice parameter  $a = 5.65 \text{ \AA}$ . In Fig. 3(d) it can be observed a small silver drop on the tip of a nanowire and in Fig. 3(f) a small indium drop which was on the tip of a nanowire (and released during HRTEM analysis), both confirming the VLS growing mechanism. Similar results were found for GeNWs grown using Au, Cu and Ni.

EDS analyses of the nanowires, depicted in Fig. 4(a), show that they are really composed by germanium; also, they showed that no significant amount of catalyst metal (Ag, In or Ni) was present along the nanowire (or it is below the detection limit of the equipment), as well as any other element. Once the HRTEM images and corresponding FFT patterns did not show any germanium oxide, the small oxygen peak can be related to the presence of this element in the atmosphere. The Si and Cu small peaks refer to the residues of substrates and the support grid of HRTEM equipment.

For micro-Raman analyses, at least five individual nanowires were picked up from Si/SiO<sub>2</sub> synthesis substrates and were put in quartz substrates. In this setup the laser used as excitation was focused to a spot size with diameter smaller than 1  $\mu\text{m}$ . For measurements, the power of laser was reduced to below 800  $\mu\text{W}$ , preventing heating or damage to the samples. The Raman spectra of all individual nanowires grown from Ag, Cu, In and Ni are similar and present peaks associated to the quartz substrates and a peak in vicinity of 300  $\text{cm}^{-1}$ , attributed to Ge optical phonons, as shown in Fig. 4(b). The Raman spectra, as well as HRTEM images and FFTs, do not indicate the presence of germanium oxide in the individual nanowires; so it should be located at the microcrystals on the growth substrates.

More structural information can be attained by performing a quantitative analysis of the germanium peak on these spectral features. When the translational invariance is destroyed by the presence of crystalline imperfections or finite size effects, phonons

will be localized describing correlation lengths corresponding to the extensions of the regions which present crystalline order. The decrease in the uncertainty of the localization of the phonons implies in the increasing of the uncertainties of their momenta, and a consequent breakdown in the selection rule for the momentum conservation, allowing the contribution of excitations with  $q > 0$  to the Raman intensity. If we are dealing with phonons with negative dispersion relation (as in the case of optical phonons in germanium), in the presence of a strong localization, the contribution of phonons with lower wavenumbers will result in a spectral line redshifted and broadened towards lower wavenumbers. The inset in Fig. 4(b) shows the theoretical Raman spectra in the region of Ge optical vibrations, considering several phonon localization lengths ( $L_{\text{ph}}$ ). The calculations were performed using the spatial correlation model [18]. The phonon dispersion relations of germanium used in our calculations were taken from Ref. [19]. For phonon localization length larger than 20 nm no significant redshift or asymmetry can be noticed, and resulting Raman lines present symmetric shapes and equal central positions. Thus, this value can be assumed as the upper limit for the phonons localization length which produces significant modifications in the Raman spectra.

Phonon localization effects were examined in our nanowires by fitting each experimental spectrum with a correspondent theoretical line calculated with spatial correlation model. Since  $L_{\text{ph}}$  is the only adjustable parameter, this procedure led to the determination of phonon localization length in each nanowires sample.

As examples, open circles in Fig. 4(c) show the Raman spectra measured individually from nanowires grown using In (top) and Ni (bottom). The spectra taken from nanowires grown with In are quite similar with respect to the position and width of the peaks. None of these spectra can be fitted using  $L_{\text{ph}}$  values lower than 20 nm, as an indication that in these nanowires the optical phonons are not localized by the presence of any type of structural disorder, but rather propagate describing large correlation lengths in all directions. The same occurs with the nanowires grown using Cu [20] and Ag. These results express the high crystalline quality of the nanowires.

On the other hand, each spectrum measured from Ni-seeded nanowires clearly differs both in energy and broadening. The fitting of the experimental data led to different values of phonon localization lengths around 10 nm, which are compatible with the

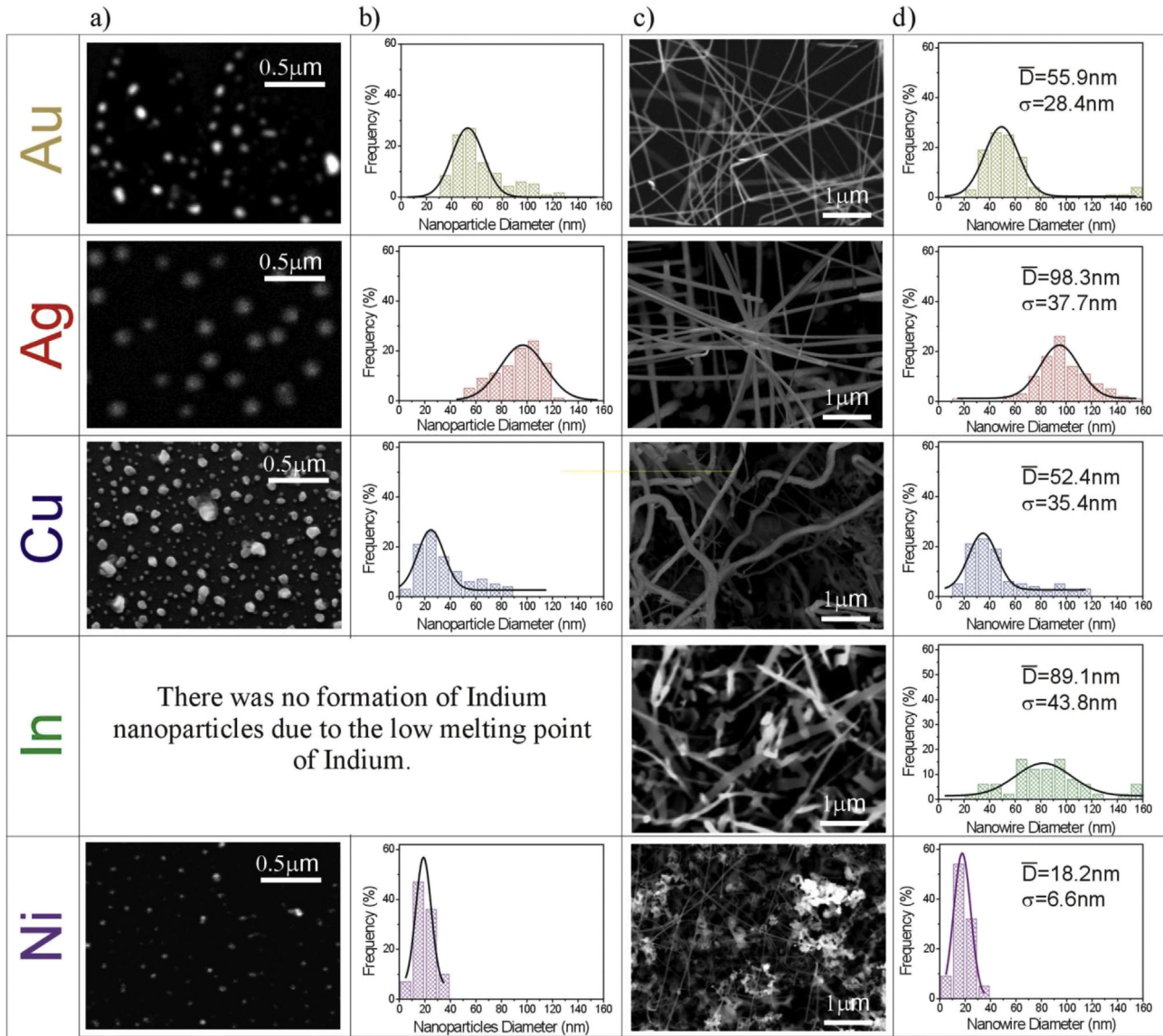


**Fig. 2.** SEM and FESEM images of: a) Au, Ag, Cu and Ni nanoparticles used as nucleation seeds and c) GeNWs grown from different metal catalysts; Histograms of the distribution of: b) nanoparticle diameters and d) germanium nanowire diameters.

diameters histogram depicted in Fig. 2. These results also confirm the high crystallinity of the wires, since the phonon localization is not related to the presence of structural disorder, but is a consequence of the confinement of the phonons due to the diameters finite size.

Therefore, the analyses of individual nanowires have confirmed the fact that the metal used as catalyst did not affect the composition or the crystal structure of the nanowires, once the results of the various and different samples were similar. These results also revealed the effect of phonon localization in the nanowires grown using nickel as catalyst, which appeared as a consequence of the difference in the dimensions of the nanowires.

#### 4. Transport mechanism in the nanowire network devices

Although the catalyst seeds have not influence remarkably neither the nanowire composition nor the crystalline quality, they possibly alter electrical characteristics. Thus, aiming the study of the influence of the catalysts on nanowires electronic behavior is

also important to verify the effects on transport mechanisms induced by the metal seeds.

For simplicity, nanowire network devices used for electrical characterization were built by evaporating metallic contacts (Au, Ag or Ti, 80 nm thick) on the Si/SiO<sub>2</sub> substrates where nanowires were grown, as depicted in inset of Fig. 5(b). Transport measurements were carried out using an electrometer (Keithley 6517) and a closed-cycle helium cryostat (Janis CCS 400H) working at a pressure lower than 10<sup>-5</sup>mbar.

Temperature-dependent resistance curves for all devices revealed the semiconductor character of the samples showing an exponential decrease of the resistance as the temperature increases. However the observed behavior did not follow the usual thermal excitation law for semiconductors [21] and thus, a more detailed investigation of the carrier transport process is required.

In real semiconductors, even when they exhibit high crystalline quality, there are invariably defects that introduces some degree of disorder [22] which interrupts the periodicity of the crystalline potential leading to localized behavior of carriers [23]. A typical

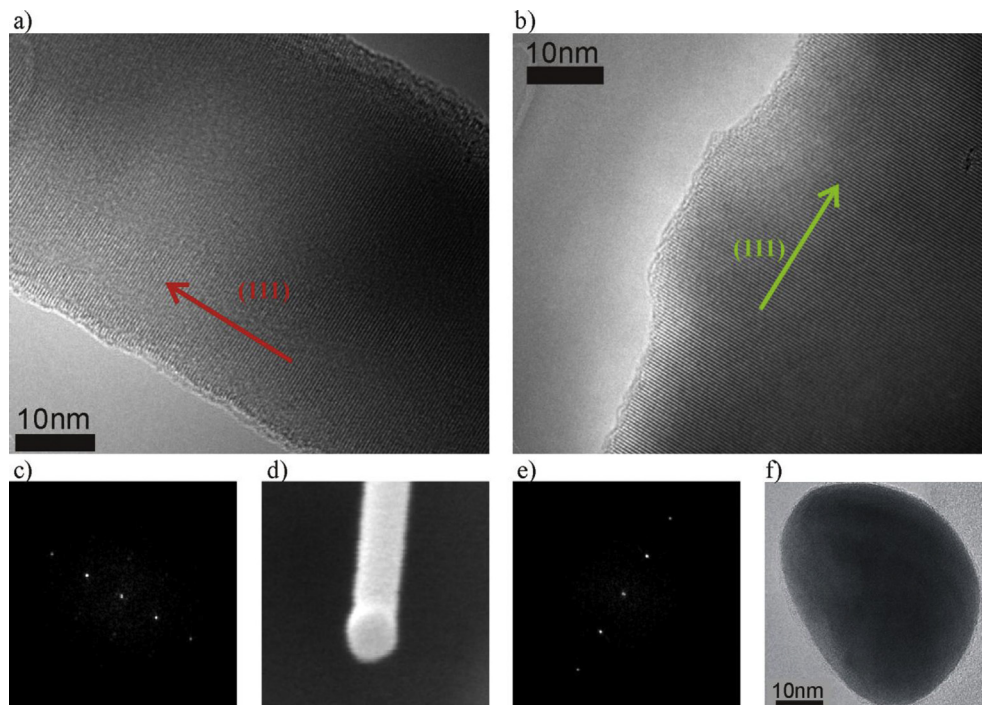


**Fig. 3.** a) HRTEM image of GeNW grown using Ag as catalyst metal; b) HRTEM image of GeNW grown using In as catalyst metal; c) FFT of GeNW depicted in (a); d) Small metal drop on the tip of a nanowire grown from silver nanoparticle; e) FFT of GeNW depicted in (b); f) Small metal drop which was on the tip of a nanowire grown using indium catalyst.

defect in crystalline materials is caused by impurities [22] which, in the synthesis by VLS method, can arise from the diffusion of the catalyst metal through the nanowire during the crystal growth process.

A mechanism of carrier transport observed in semiconductor in which the disorder is not strong is the variable range hopping (VRH) originally due to Mott and described by

$$\rho(T) = \rho_0 \exp\left(\frac{T_0}{T}\right)^{\frac{1}{4}} \quad (1)$$

where  $\rho_0$  and  $T_0$  are constants [22]. This model can be explained by the presence of localized energy levels around Fermi level that trap carriers and the transport occurs as a result of carriers hopping from an occupied to a free localized state.

The temperature dependent resistance measurements obtained from several devices (nanowires grown using the five catalyst metals) are depicted in Fig. 5(a). The data presented a good agreement with the VRH process which can be considered the main transport mechanism in all measured GeNWs.

According to Mott's model [24] it is also possible to calculate the hopping range ( $R_{\text{hopping}}$ ) by

$$R_{\text{hopping}}(T) = \left[ \frac{3}{2 \pi N k T} \left( \frac{7,6}{T_0 N k} \right)^{\frac{1}{3}} \right]^{\frac{1}{4}} \quad (2)$$

where  $k$  is Boltzmann constant and  $N$  is the density of states at the Fermi level. Mean values of  $R_{\text{hopping}}$  at room temperature ( $T = 300$  K) for several devices are plotted in Fig. 5(b). Similar results were found for all catalyst seeds, around 4.5 nm, and this value corresponds to the distance that electrons must hop in order to contribute to the conductivity.

Despite the differences in properties of metal catalyst, like diffusion coefficients or possible energy levels as impurities in

germanium [25], the nanowires grown from Au, Ag, Cu, In and Ni presented similar electronic behavior, for both transport mechanism and hopping distance. Even showing long range order in crystalline structure, an electronic disorder makes VRH the main transport mechanism. On the other hand, the uniformity of  $R_{\text{hopping}}$  suggests that the energy levels, which could be created by the catalysts, are not the localized states that dominate the transport in germanium nanowires. Considering that the structural characterization did not show significant crystalline disorder in the volume of the nanowires along with previously results found by other techniques for Au-catalyst GeNWs [26], the disorder was probably generated by surface states.

## 5. Conclusion

Summarizing, this work shows that is possible to grow single crystalline GeNWs by VLS method using different catalyst metals – Au, Ag, Cu, In and Ni, only adjusting the synthesis temperature. Preliminary studies revealed that the nanowires diameters and diameters distribution were compatible with the characteristics of the nanoparticles generated by thermal treatment of metallic thin films; for Ni-based germanium nanowires, the reduced diameter of the samples leads to phonon localization effects, as demonstrated in Raman spectroscopy. X-ray patterns, HRTEM images, EDS and Raman spectroscopy showed nanowires composed by germanium and presenting crystalline long range order, independent of the catalyst metal used in the synthesis. Although the structural regularity, electrical analysis performed on GeNWs network devices demonstrated that VRH was the main transport mechanism, indicating that a small disorder in electronic potential dominates the carrier transport; nevertheless, the fitting of experimental data with VRH model found hopping distances around 4.5 nm for the different devices suggesting that the catalyst was not responsible for electrical disorder.

These results, specially the high germanium crystalline quality

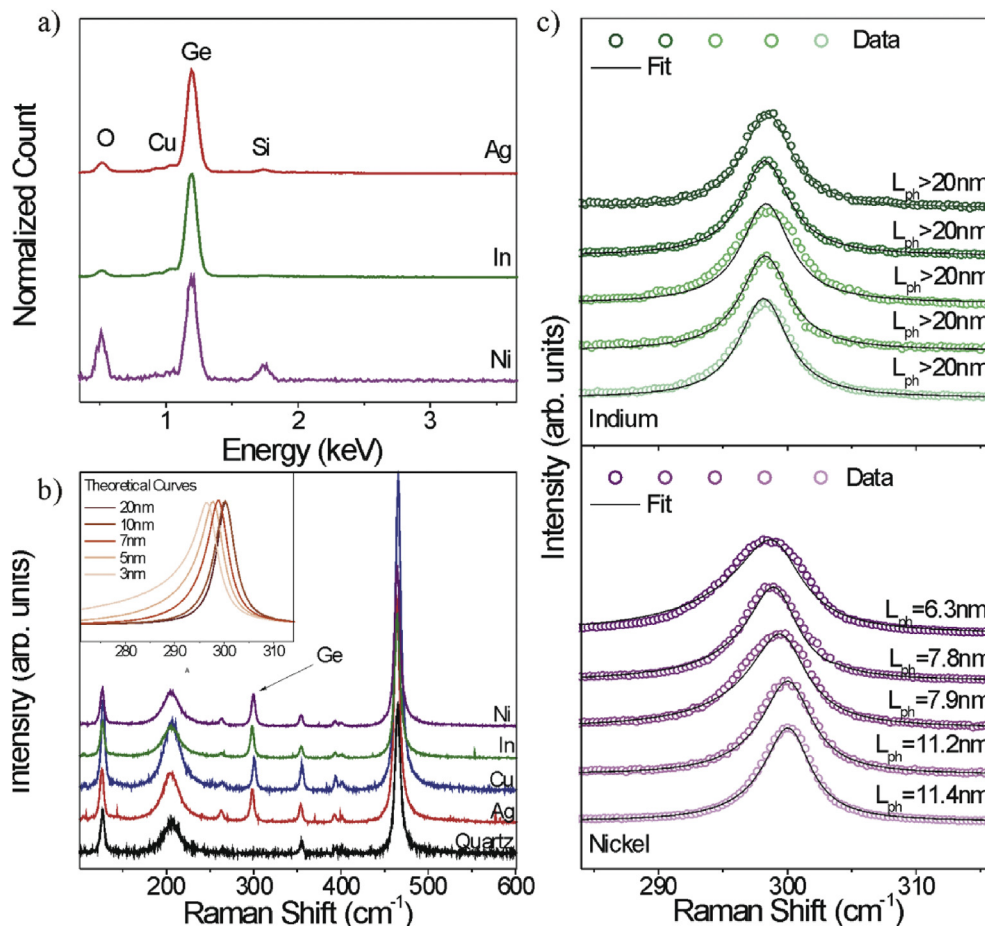


**Fig. 4.** (a) EDS spectra of GeNWs grown using Ag, In and Ni as catalysts; (b) Raman spectra of individual nanowires grown using Ag, Cu, In and Ni as catalysts showing only the Ge peak, beyond the peaks related to the quartz substrate. Inset: Theoretical Raman spectra in the range of germanium optical vibrations, calculated using the spatial correlation model with different phonon localization lengths; (c) Raman spectra of five individual In-seeded (top) and Ni-seeded (bottom) nanowires showing experimental data Ge peaks (dots) adjusted to the theoretical spectra (straight lines).

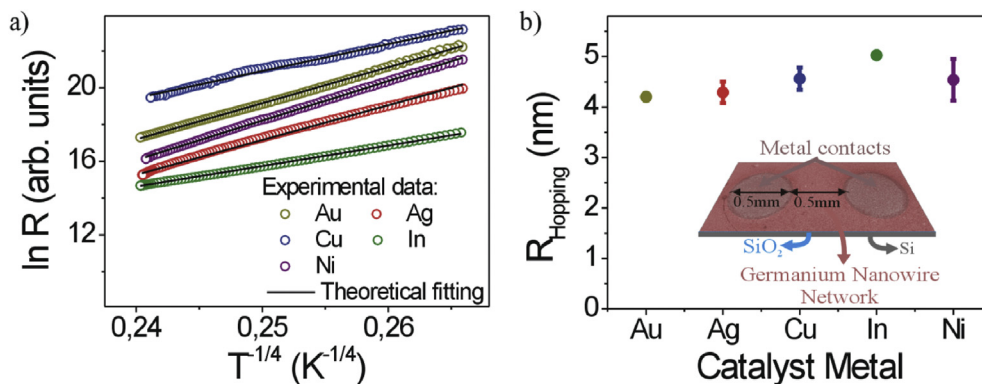


**Fig. 5.** a) Temperature-dependent resistance data of GeNWs devices fitted with VRH transport mechanism model. b) Mean values of  $R_{\text{hopping}}$  distance for several devices, with their respective standard deviations; in the inset, is shown a sketch of germanium nanowire network devices.

and the similarities of electrical properties of the nanowires grown using all catalyst metals investigated, allow the choice of a particular catalyst based on the characteristics of the laboratory equipments that will produce the nanowires - range of temperature of synthesis furnace, for example - or on the applications, with the selection of desired diameters or availability and cost of the metal.

#### Acknowledgments

We thank the Brazilian research funding agencies under grants 2012/06916-4, São Paulo Research Foundation (FAPESP) and 302640/2010-0 and 471086/2013-4 (CNPq) for the supporting of this work.

## References

- [1] R.G. Hobbs, N. Petkov, J.D. Holmes, Semiconductor nanowire fabrication by bottom-up and top-down paradigms, *Chem. Mater.* 24 (2012) 1975–1991.
- [2] G. Gu, M. Burghard, G.T. Kim, G.S. Dusberg, P.W. Chiu, V. Krstic, S. Roth, Growth and electrical transport of germanium nanowires, *J. Appl. Phys.* 90–11 (2001) 5747–5751.
- [3] P. Artoni, A. Irrera, E.F. Pecora, S. Boninelli, C. Spinella, F. Priolo, Hetero-epitaxial growth of Ge nanowires on Si substrates, *Int. J. Photoenergy* 2012 (2012) 782835.
- [4] C. O'Regan, S. Biswas, N. Petkov, J.D. Holmes, Recent advances in the growth of germanium nanowires: synthesis, growth dynamics and morphology control, *J. Mater. Chem. C* 2 (2014) 14–33.
- [5] X.H. Sun, C. Didychuk, T.K. Shamand, N.B. Wong, Germanium nanowires: synthesis, morphology and local structures studies, *Nanotechnology* 17 (2006) 2925–2930.
- [6] H. Kamimura, L.S. Araujo, O.M. Berengue, C.A. Amorim, A.J. Chiquito, Growth and electrical characterization of semiconducting Ge nanowires, *Phys. E* 44 (2012) 1776–1779.
- [7] S. Barth, J.J. Boland, J.D. Holmes, Defect transfer from nanoparticles to nanowires, *Nano Lett.* 11 (2011) 1055–1550.
- [8] S. Biswas, A. Singha, M.A. Morris, J.D. Holmes, Inherent control of growth, morphology, and defect formation in germanium nanowires, *Nano Lett.* 12 (2012) 5654–5663.
- [9] K. Kang, D.A. Kim, H.S. Lee, C.J. Kim, J.E. Yang, M.H. Jo, Low-temperature deterministic growth of Ge nanowires using Cu solid catalyst, *Adv. Mater.* 20 (2008) 4684–4690.
- [10] H. Geaney, C. Dickinson, C.A. Barrett, K.M. Ryan, High density germanium nanowire growth directly from copper foil by self-induced solid seeding, *Chem. Mater.* 23 (2008) 4838–4843.
- [11] X. Lu, J.T. Harris, J.E. Villarreal, A.M. Chockla, B.A. Korgel, Enhanced nickel-seeded synthesis of germanium nanowires, *Chem. Mater.* 25 (2013) 2172–2177.
- [12] S.V. Thombare, A.F. Marshall, P.C. McIntyre, Kinetics of germanium nanowire growth by de the vapor-solid-solid mechanism with Ni-based catalyst, *Appl. Mater.* 1 (2013) 061101.
- [13] Y. Xiang, L. Cao, S. Conesa-Boj, S. Estrade, J. Arbiol, F. Peiro, M. Hei, I. Zardo, J.R. Morante, M.L. Brongersma, A.F.I. Morral, Single Crystalline and core-shell indium-catalyzed germanium nanowires—a systematic thermal CVD growth study, *Nanotechnology* 20 (2009) 245608.
- [14] Joint Committee on Powder Diffraction Standards (JCPDS), Card No. 4–545.
- [15] Joint Committee on Powder Diffraction Standards (JCPDS), Card No. 36–1463.
- [16] T.P. Mernagh, L.-G. Liu, Temperature dependence of Raman spectra of the quartz and rutile-types of GeO<sub>2</sub>, *Phys. Chem. Miner.* 24 (1997) 7–16.
- [17] G. Cao, *Nanostructures and Nanomaterials: Synthesis, Properties and Applications*, Imperial College Press, London, 2004.
- [18] I.H. Campbell, P.M. Fauchet, The effects of microcrystal size and shape on the one phonon Raman spectra of crystalline semiconductors, *Solid State Commun.* 58 (1986) 739–741.
- [19] P. Giannozzi, S. Gironcoli, P. Pavone, S. Baroni, Ab initio calculation of phonon dispersions in semiconductors, *Phys. Rev. B* 43–9 (1986) 7231–7242.
- [20] R.C. Gouveia, H. Kamimura, R. Munhoz, A. de, G. Rodrigues, E.R. Leite, A.J. Chiquito, Characterization of germanium nanowires synthesized using copper as catalyst metal, *Quim. Nova* 38–6 (2015) 777–780.
- [21] P. Yu, M. Cardona, *Fundamentals of Semiconductors*, Springer, Berlin, 2010.
- [22] J. Singh, *Smart Electronic Materials: Fundamentals and Applications*, Cambridge University Press, Cambridge, 2005.
- [23] R.A. Simon, H. Kamimura, O.M. Berengue, E.R. Leite, A.J. Chiquito, Disorder induced interface states and their influence on the Al/Ge nanowires Schottky devices, *J. Appl. Phys.* 114 (2013) 243705.
- [24] N.F. Mott, E.A. Davis, *Electronic Processes in Non-crystalline Materials*, Clarendon Press, Oxford, 1979.
- [25] C. Claeys, E. Simoen, *Germanium-based Technologies: from Materials to Devices*, Elsevier, Oxford, 2007.
- [26] S. Zhang, E.R. Hemesath, D.E. Perea, E. Wijaya, J.L. Lensch-Falk, L.J. Lauhon, Relative influence of surface states and bulk impurities on the electrical properties of Ge nanowires, *Nanoletters* 9–9 (2009) 3268–3274.